Article

Numerical and Experimental Study of Lightning Stroke to BIPV Modules

Xiaoyan Bian [1], Yao Zhang [1], Qibin Zhou [1,2,*], Ting Cao [2] and Bengang Wei [3]

1   College of Electrical Engineering, Shanghai University of Electric Power, Shanghai 200090, China;
    bianxy@shiep.edu.cn (X.B.); zhangyao8253@163.com (Y.Z.)
2   School of Mechatronic Engineering and Automation, Shanghai University, Shanghai 200444, China;
    15102348682@163.com
3   State Grid Shanghai Municipal Electric Power Company, Shanghai 200122, China; wbgsj@126.com
*   Correspondence: zhouqibin@shu.edu.cn; Tel.: +86-138-1779-0981

Abstract: Building Integrated Photovoltaic (BIPV) modules are a new type of photovoltaic (PV) modules that are widely used in distributed PV stations on the roof of buildings for power generation. Due to the high installation location, BIPV modules suffer from lightning hazard greatly. In order to evaluate the risk of lightning stroke and consequent damage to BIPV modules, the studies on the lightning attachment characteristics and the lightning energy withstand capability are conducted, respectively, based on numerical and experimental methods in this paper. In the study of lightning attachment characteristics, the numerical simulation results show that it is easier for the charges to concentrate on the upper edge of the BIPV metal frame. Therefore, the electric field strength at the upper edge is enhanced to emit upward leaders and attract the lightning downward leaders. The conclusion is verified through the long-gap discharge experiment in a high voltage lab. From the experimental study of multi-discharge in the lab, it is found that the lightning interception efficiency of the BIPV module is improved by 114% compared with the traditional PV modules. In the study of lightning energy withstand capability, a thermoelectric coupling model is established. With this model, the potential, current and temperature can be calculated in the multi-physical field numerical simulation. The results show that the maximum temperature of the metal frame increases by 16.07 °C when 100 kA lightning current flows through it and does not bring any damage to the PV modules. The numerical results have a good consistency with the experimental study results obtained from the 100 kA impulse current experiment in the lab.

Keywords: building integrated photovoltaic (BIPV); lightning attachment characteristics; lightning energy withstand capability; numerical and experimental analysis

1. Introduction

As a new form of clear power generation, photovoltaic (PV) power generation has attracted more and more attention around the world. Currently, first and second-generation PV technologies are already included for building integration photovoltaic (BIPV) and building attached/applied photovoltaic (BAPV) application in the form of roof, window, wall and shading elements. In addition, third-generation PVs are under exploration [1–3]. With BIPV, it can not only generate power for the building consumers or even power companies, but also save cost and space when constructing the distributed PV stations on buildings. The application of BIPV modules is the development trend of green buildings. It also represents the future of urban and building energy development [4–6].

Due to the high installation location, BIPV modules suffer from lightning hazard greatly. Lightning is a natural phenomenon of a strong discharge, releasing tremendous energy. When lightning strikes BIPV, it will cause deformation and melting of metal framework and damage to PV modules [7,8]. In total, 5% to 10% of solar installations are damaged by direct lightning or lightning electromagnetic pulse every year [9].

To ensure PV systems safe and reliable, lightning protection design attracts more and more attention. At present, there is much research on direct lightning and lightning-induced overvoltage in PV power plants [10–13]. Y. G. Jia [14] and F. Y. Guo [15] pointed out the design of the green building and the key point of lightning protection. N. H. Zaini [16] simulated the lightning stroke of different waveforms and amplitudes on different parts of the photovoltaic system, and found that the transient current would appear at the nearest point to the lightning striking, while the transient voltage would appear on the AC side of the inverter. Jae-Young Cho [17] analyzed the damage of lightning overvoltage to PV array infrastructure, and considered the influence caused by different lightning striking locations and distances on PV array. C. Dechthummarong [18] studied the lightning withstand of insulation materials of field-aged PV modules, applied a pulse of 1.2/50 μs between impulse voltage generator (IVG) and PV modules, and realized the mathematical model of partial discharge in PV insulation gap. The experimental results showed that insulation defects caused by aging produce partial discharge between PV modules and aluminum frame. K. Tamura [19] conducted a lightning stroke test on a centralized PV system with an area of 75 m^2, a height of about 10 m and an installed capacity of 14 kW. The test showed that the lightning current attached the fabricated aluminum chassis and flowed into the ground, which verified the lightning energy withstand capability of centralized PV modules. K. M. Coetzer [20] conducted a lightning current test in a high voltage lab, and found that poor wiring between PV modules leads to the arising of the excessive induced current. Then, a better wiring method was proposed to reduce the amplitude of the induced current.

As an important part of the integrated roof, the BIPV modules face the threat of direct lightning strike. The configuration of BIPV is quite different from the traditional PV modules which are installed on the fixed PV brackets on the roof. However, the PV modules of BIPV are integrated with the metallic roof without any PV bracket. It changes the relative position between PV modules and surrounding metallic structures compared to the traditional PV modules. Therefore, the study of traditional PV modules is not available for BIPV directly. The study of lightning stroke to BIPV modules is very little addressed nowadays.

In order to protect BIPV modules against lightning damage, a study about the lightning stroke to BIPV modules is conducted with numerical and experimental methods in this paper. Since lightning effect to BIPV modules can be divided into two aspects, i.e., lightning attachment and lightning energy withstand, the study is also divided into two parts, the attachment characteristics in Section 2 and the energy withstand capability in Section 3 of this paper. The study conclusions of this paper will be guidance for the lightning protection of BIPV modules used in rapidly growing distributed PV stations. It would be expected that the combination of PV and building is one of the most important areas for future PV applications. It improves the lightning protection requirements of green buildings and PV systems.

2. Study of Lightning Attachment Characteristics to BIPV Modules

2.1. Numerical Simulation and Analysis

2.1.1. Modeling of Lightning Stroke to BIPV Modules

During a thunderstorm, the lightning downward leaders develop step by step from the cloud to the ground. As the lightning downward leaders approach to the ground, upward leaders will be generated when the electric field strength of the object on the ground reaches a certain level. Once the downward leader connects with the upward leader from a certain object such as BIPV modules on a building, the object will be struck by the lightning, as Figure 1 shows.
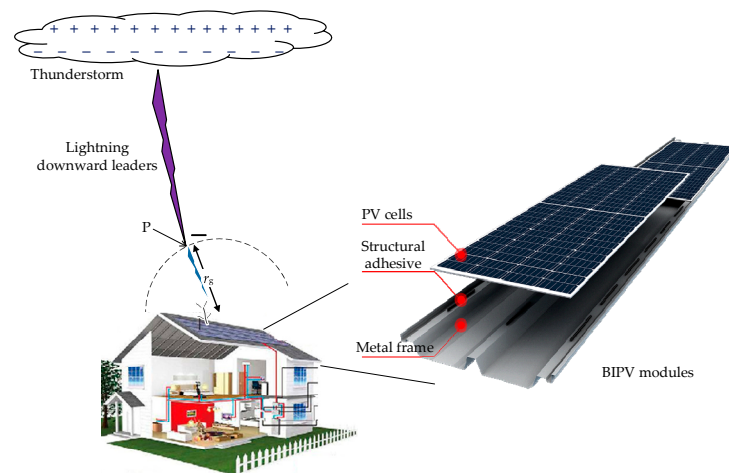
Figure 1. Schematic diagram of lightning stroke to building integration photovoltaic (BIPV) modules.

The connection is dependent on the distance between the downward leader and the upward leader reaching the breakdown threshold of the electric field. This threshold is defined as the lightning striking distance which can be interpreted as a function of lightning current, as Equations (1) and (2) shows.

$$r_c = KI_P^b \tag{1}$$

where r_c is the lightning striking distance, m; I_P is the amplitude of lightning current, kA; K and b are coefficients to account for different striking distances to a mast, a shield wire, or the ground plane [21].

According to buildings or transmission lines at different altitudes, scholars have carried out a lot of research on the three important parameters of the striking distance [22–27]. The lightning distance r_g should be corrected by Equation (2). The specific values of the lightning striking distance parameters from different literature are listed in Table 1.

$$r_g = K_g r_c \tag{2}$$

K_g is the correction factor to correct the striking distance r_c of the earth; r_g is the corrected lightning distance.

Table 1. Striking distance parameters from different literatures.

| Literature	K	b	Kg
Golde [22]	3.30	0.78	1
Young [23]	27.00	0.32	1 (h < 18); 444/(462-h)(h > 18)
Love [24]	10.00	0.65	1
Whitehead [25]	9.4	0.67	1
Anderson [26]	8.00	0.65	0.64 (EHV lines); 0.8 (UHV lines); 1 (other lines)
IEEE std 2012 [27]	8	0.65	1

According to the striking distance parameters given in IEEE Std 998-2012 [27], where $K = 8$, $b = 0.65$, $K_g = 1$. Because 50% of current amplitude $I_P = 30$ kA [28], the lightning striking distance r_g is calculated to be 73 m.

The downward leader is simplified as a rod electrode when studying the lightning striking position. The electrode voltage is taken as 50% breakdown voltage of negative lightning discharge of the rod–rod gap in air. According to Equation (3), the electrode voltage is set as 43.9 MV.

$$U_{50\%} = 110 + 6d \tag{3}$$

where $U_{50\%}$ is 50% breakdown voltage of lightning impulse, kV. d is the distance between poles, cm.

In the FEA software, an electrostatic field model of PV modules is established under lightning downward leader. As shown in Figure 2, the downward leader head is equivalent to a rod electrode, and the relative spatial distance between the rod electrode and the PV module is r_g. The PV module consists of an inner solar cells and an outer metal frame as Figure 1 shows. The material of metal frame is set to aluminum. The material of solar cells is set to silicon. Moreover, the metal frame is set to zero potential as grounding. The lightning interception position of different PV modules can be determined by evaluating the distribution of static electric field strength on the PV modules. The position with the maximum field strength is prone to be struck with maximum possibility.
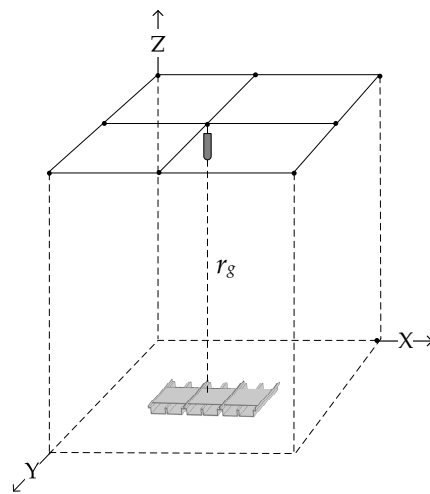
Figure 2. Simulation model of photovoltaic (PV) module under electrostatic field.

2.1.2. Electrostatic Field Theory

The electric field, due to a given charged lightning stepped leader, can be calculated using Equations (4)–(7) of electrostatics.

$$\nabla \times \boldsymbol{E} = 0 \tag{4}$$

$$\nabla \bullet \boldsymbol{D} = \rho \tag{5}$$

$$\boldsymbol{E} = -\nabla \varphi \tag{6}$$

$$\nabla^2 \varphi = -\frac{\rho}{\varepsilon} \tag{7}$$

where $\boldsymbol{E}$ is the electric field tensor; $\boldsymbol{D}$ is the electric displacement vector; ρ is the charge density; φ is the electric potential; and ε is the permittivity of the free space.

It should be noted that the lightning distance r_g determines the relative spatial position between the lightning downward leader and BIPV modules in the computational domain, and also determines the locations of the zero-electric potential boundary conditions that are associated with the metal frame.

2.1.3. Simulation Results and Analysis

The FEA software is used to solve the governing Equations (4)–(7). As shown in Figure 3a, the sharp corners of metal frame are easy to accumulate charges. The maximum surface charge density is 140 μc/m^2. The minimum surface charge density is 6.89 μc/m^2. As shown in Figure 3b, charges are more likely to accumulate on the border of BIPV modules, with the maximum surface charge density of 194 μc/m^2 and the minimum surface charge density of 0.11 μc/m^2. In the electrostatic field formed by the lightning downward leader head, the space charge accumulates on the surface of the ground object

leading to the electric field. The upper edge of metal frame is easier to gather charges which can enhance electric field intensity.
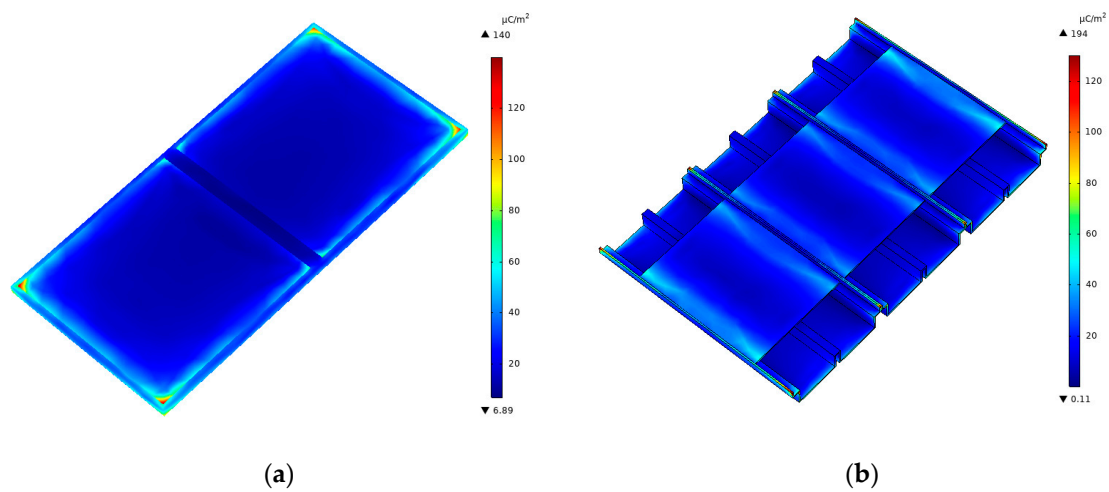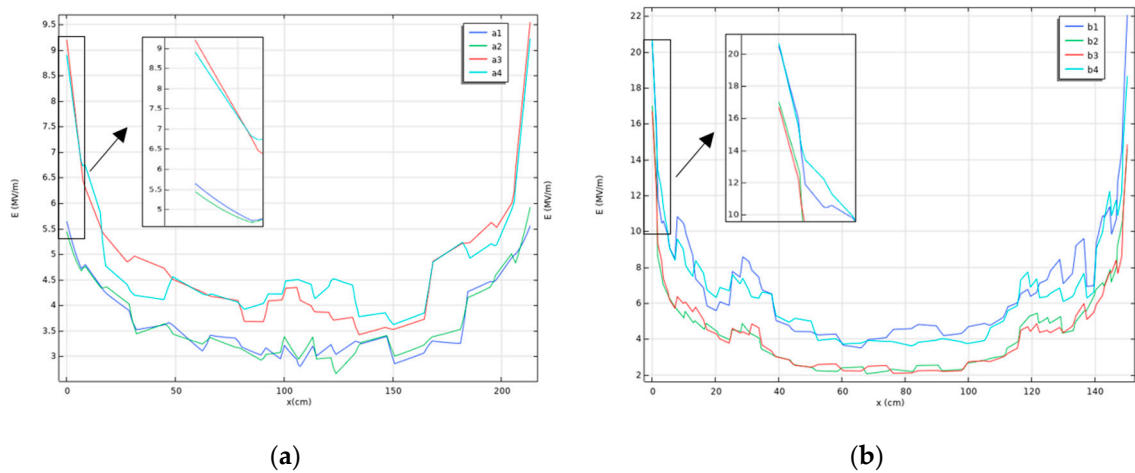

Figure 3. Surface charge density of two PV modules (**a**) framed double-glass PV module; (**b**) BIPV module unit combination.

Through numerical calculation, the surface electric field strength distribution of the two PV modules is shown in Figure 4. It can be seen that the highest electric field strength of framed double-glass PV module is distributed at the four corners of the metal frame. The highest field strength of BIPV module is distributed on the upper edge of metal frame. In addition, the electric field strength on the two metal frames is much higher than that of the internal solar cells.
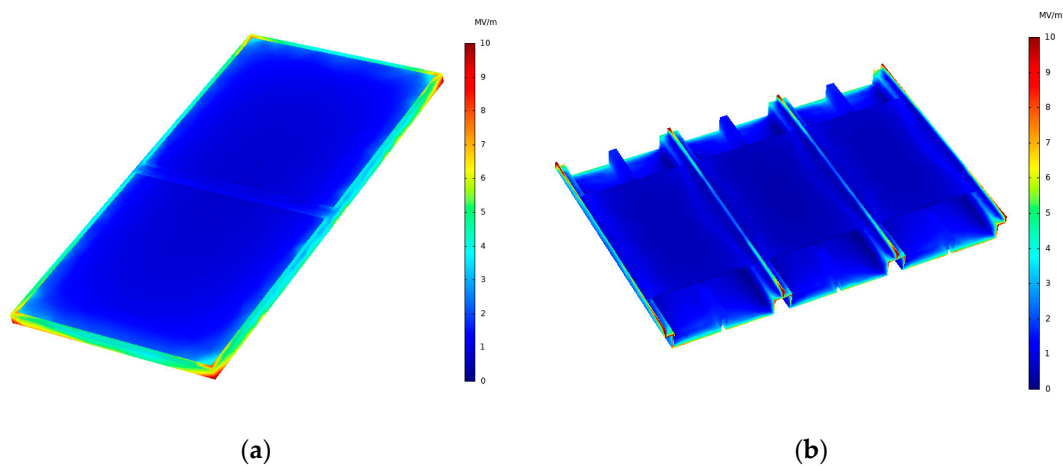
Figure 4. Surface electric field strength of different PV modules (**a**) framed double-glass PV module; (**b**) BIPV module unit combination.

Take different paths along the arrow direction on the metal frame, defined as a1–a4 and b1–b4. The measured electric field strength along different paths is shown in Figure 5. The maximum electric field strength is distributed at both ends of the metal frame. Those on the surfaces of framed double-glass PV module and BIPV module is 9.5 MV/m and 22.1 MV/m respectively. The electric field strength is increased by 132%. The locations of the PV modules surface with higher electric field strength are considered to have higher possibility of emitting answering leaders and intercepting the lightning stepped leader.

(**a**)   (**b**)

Figure 5. Distribution of surface electric field strength (**a**) framed double-glass PV module; (**b**) BIPV module unit combination.

2.2. Experimental Study

2.2.1. Sample Preparation

In order to compare the different lightning protection performance of various PV modules and verify the accuracy of the simulation, three experimental samples were selected according to the models in the numerical simulation in Section 2.1. As shown in Figure 6a, a 213 cm × 105 cm framed double-glass PV module was selected as a counterpart piece and defined as Sample A, which was assembled by the metal frame and solar cells. At the same time, a 222 cm × 150 cm BIPV module unit combination was defined as Sample B, as shown in Figure 6b. In the lightning current withstand capability test in Section 3.2, the BIPV module unit with metal frame of 150 cm × 72.5 cm was selected for the test, which is defined as Sample C, as shown in Figure 6c.
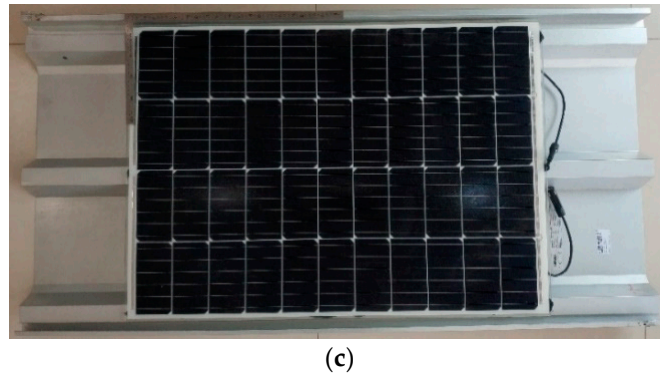

(**a**)   (**b**)

Figure 6. *Cont.*

(**c**)

Figure 6. Experimental samples (**a**) framed double-glass PV module; (**b**) BIPV module unit combination; (**c**) BIPV module unit.

2.2.2. Experimental Method

In order to simulate the lightning stroke of PV modules under thunderstorm clouds, an experimental platform was set up in the high voltage laboratory. The long gap discharge of PV module by SJTU-3000 impulse voltage generator (IVG) was used to simulate the spatial potential and electric field distribution of PV modules during the scene of lightning downward leader descending process.

The schematic diagram of the experimental platform is shown in Figure 7a. Place Sample A and Sample B horizontally on the ground. Keep the metal frame well grounded. The rod electrode connected with SJTU-3000 IVG was located directly above the center of PV modules, with a vertical distance of 2 m. The layout of the experimental platform is shown in Figure 7b. As more than 90% of lightning in nature is negative, SJTU-3000 IVG was used to apply negative lightning impulse voltage with 1.2/50 μs waveform for 20 times. In order to prevent the subsequent experiment from being affected by the breakdown of the solar cells, the solar cells surface of the experimental sample was covered with 5 mm thick glass. Moreover, the insulation blanket was used to cover the sharp corners to prevent lightning striking at these corners because these sharp corners do not exit when BIPV is installed on the building roof. Therefore, the influence of glass and insulating blanket on this test can be ignored. After each discharge, the location of lightning striking attachment point was recorded to calculate the lightning striking attachment probability of the samples, with the lightning protection effect of different PV modules evaluated.

(**a**)

(**b**)
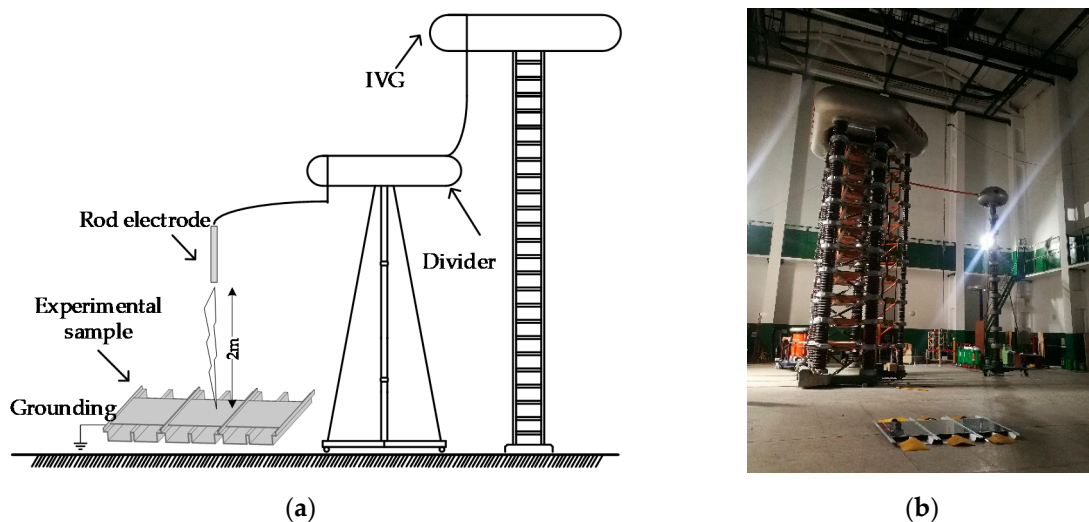
Figure 7. Lightning attachment experiment (**a**) Schematic diagram of experimental platform; (**b**) Layout of experimental setup.

2.2.3. Experimental Results and Analysis

According to the experiment method in Section 2.2.2, the long gap arc was attached to the metal frame of Sample A seven times. The arc was attached to the solar cells and flashed over the surface to the metal frame 13 times. Consequently, the interception efficiency of the metal frame was 35%. Figure 8a,b show the successful and failed interception of the discharge arc of Sample A. Under the same experimental conditions, it was noted that the arc attached to the metal frame of Sample B for 15 times. The other five discharge arcs flashed over the surface of solar cells. Then the interception efficiency is 75%. Figure 8c,d show the successful and failed interception of the discharge arc of Sample B. Compared with the electric field distribution and the experimental results, the location of lightning attachment point is very close to simulation results in Section 2.1.3, which can be used to check the effectiveness of the simulation method.

(**a**)

(**b**)

(**c**)

(**d**)
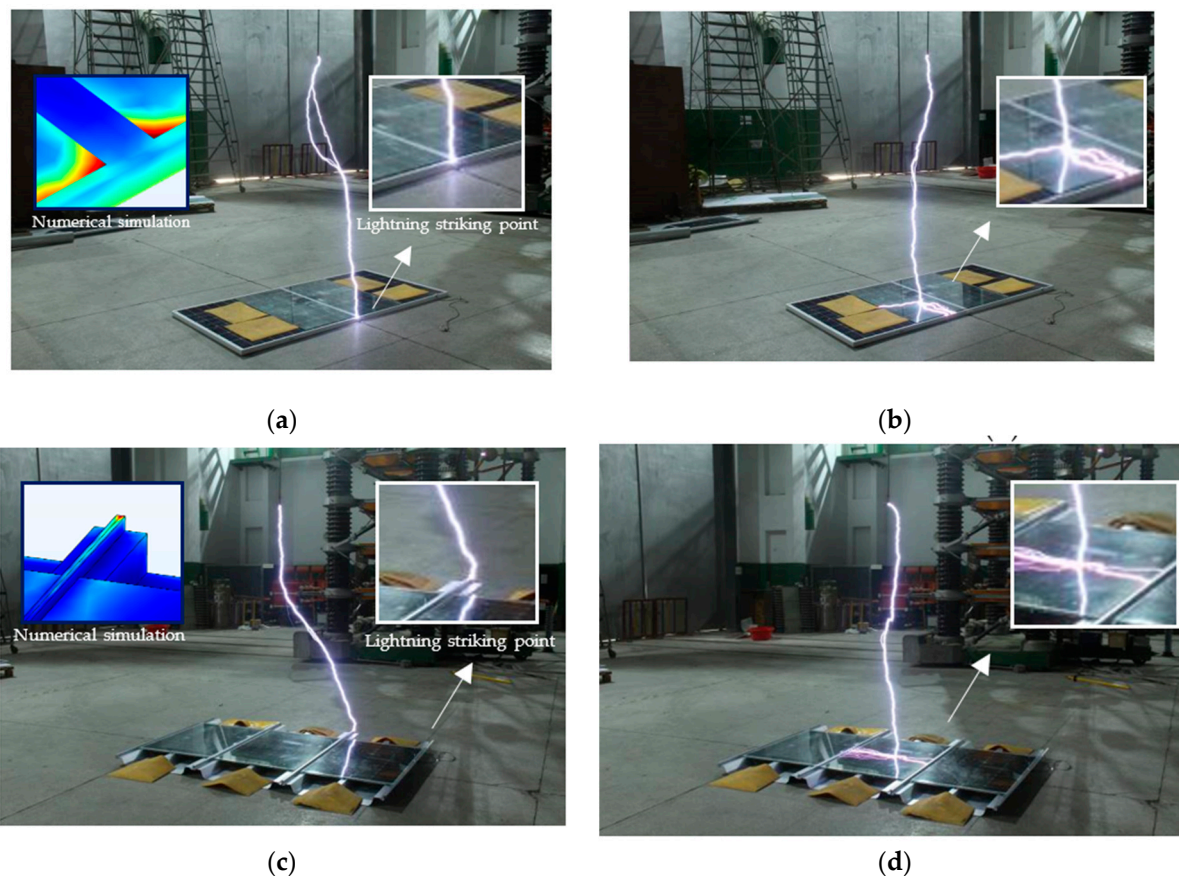
Figure 8. Lightning connection of different PV modules (**a**) Lightning connection of metal frame of Sample A; (**b**) Surface flashover of Sample A; (**c**) Lightning connection of metal frame of Sample B; (**d**) Surface flashover of Sample B.

It is noted that under the impulse 1.2/50 μs standard lightning voltage, the metal frame of Sample B was easier to attract the discharge arc generated by the rod electrode than the metal frame of Sample A. The interception efficiency is increased by 114%. That is to say, the metal frame of the BIPV module has better lightning interception performance, which can protect the solar cells from lightning damage more effectively.

3. Study of Lightning Energy Withstand Capability to BIPV Modules

3.1. Numerical Simulation and Analysis

3.1.1. Thermoelectric Coupling Theory

In the process of flowing through BIPV modules, lightning current converted to Joule heat acts on BIPV modules. Studying the temperature field distribution plays a crucial role in the lightning energy withstand capability of BIPV modules. In this section, the

thermoelectric coupling analysis model of BIPV modules is established. The solution of the model is based on the law of charge conservation and the law of conservation of energy.

According to the law of charge conservation, the governing equation of electric field in conductor is as follows,

$$\int_s \boldsymbol{J} \bullet \mathbf{n} dS = \int_v r_c dV \tag{8}$$

where S is cross sectional area of unit; V is unit volume; $\mathbf{n}$ is normal vector; $\boldsymbol{J}$ is current density; and r_c is charge density per unit volume.

Based on Ohm's law, current density can be defined as Equations (9),

$$\boldsymbol{J} = \sigma \bullet \boldsymbol{E} = -\sigma \bullet \nabla\Phi \tag{9}$$

where σ is the conductivity; $\boldsymbol{E}$ is the electric field strength; and Φ is the electrical potential.

The governing equation in the finite element is obtained as Equations (10),

$$\int \nabla\delta\Phi \bullet (\sigma \bullet \nabla\Phi)dV = \int_V \delta\Phi r_c dV + \int_S \delta\Phi \bar{J} dS \tag{10}$$

According to Joule's law, the current flowing through the conductor will be converted into Joule heat, as shown in the following relationship.

$$P_{\text{ec}} = \boldsymbol{J} \bullet \boldsymbol{E} = (\sigma \bullet \boldsymbol{E}) \bullet \boldsymbol{E} \tag{11}$$

$$r = \eta_v P_{\text{ec}} \tag{12}$$

where P_{ec} is the power loss density; η_v is the energy conversion factor; and r is the thermal density.

The governing equation of heat conduction is obtained as Equations (13),

$$\int_v \rho C_v \frac{\partial\theta}{\partial t}\partial\theta dV + \int_v \nabla\partial\theta \bullet (K \bullet \nabla\theta)dV = \int_v \delta\theta r dV + \int_s \delta\theta q dS \tag{13}$$

where θ is the temperature; K is the solid thermal conductivity; ρ is the solid density; C_v is the specific heat capacity; and q is the heat flux density.

Equations (10) and (13) describe the governing equations of thermoelectric coupling problem. When studying lightning current withstand capability of BIPV modules, the potential, current and temperature can be calculated in the multi-physical field numerical simulation.

3.1.2. Modeling of Lightning Current

The heat source was given as a large current in the multi-physical field numerical simulation model. The lightning current used in lightning transient calculation can be divided into three categories: double exponential model, Heidler model and pulse function model [29]. In 1941, Bruce and Golde put forward the double exponential function model of lightning current [30]. The concise mathematical expression can describe the typical lightning current waveform, which has been widely used in the field of lightning protection. The expression form is expressed in Equation (14).

$$i(t) = \frac{I_0}{\eta}\left(e^{-\alpha t} - e^{-\beta t}\right) \tag{14}$$

In which I_0 is the peak current; η indicates the peak correction coefficient; $\alpha = 1/T_1$, $\beta = 1/T_2$, T_1 is the wave head time and T_2 is the wave tail time.

In the simulation, the mathematical model of lightning current adopts double exponential model, the amplitude of lightning current is 10–100 kA, the peak correction coefficient is 0.998, the current waveform is 10/350 μs standard lightning wave. According

to the results of Section 2.2.3, the maximum electric field strength on the surface of PV module is set as the lightning injection point.

3.1.3. Simulation Result and Analysis

The methodology of Section 3.1.1 can be used to verify the transient state of current distribution and lightning energy withstand capability of BIPV module unit. Figure 9 shows the transient distribution of lightning current at six times. Lightning current flows from attachment point of the metal frame to the grounding point. From 0 µs to 14 µs, the current density instantly increases and reaches a peak value of 4.16×10^9 A/m^2. At the half peak time of 350 µs, the current density gradually decreases to 2.06×10^9 A/m^2, and then tends to 0. Because the simulated lightning current waveform is 10/350 µs with a short rising edge, the current density reaches the maximum in a short time. There is no current passing through the solar cells in the whole process, so it is noted that the metal frame can effectively protect the solar cells.
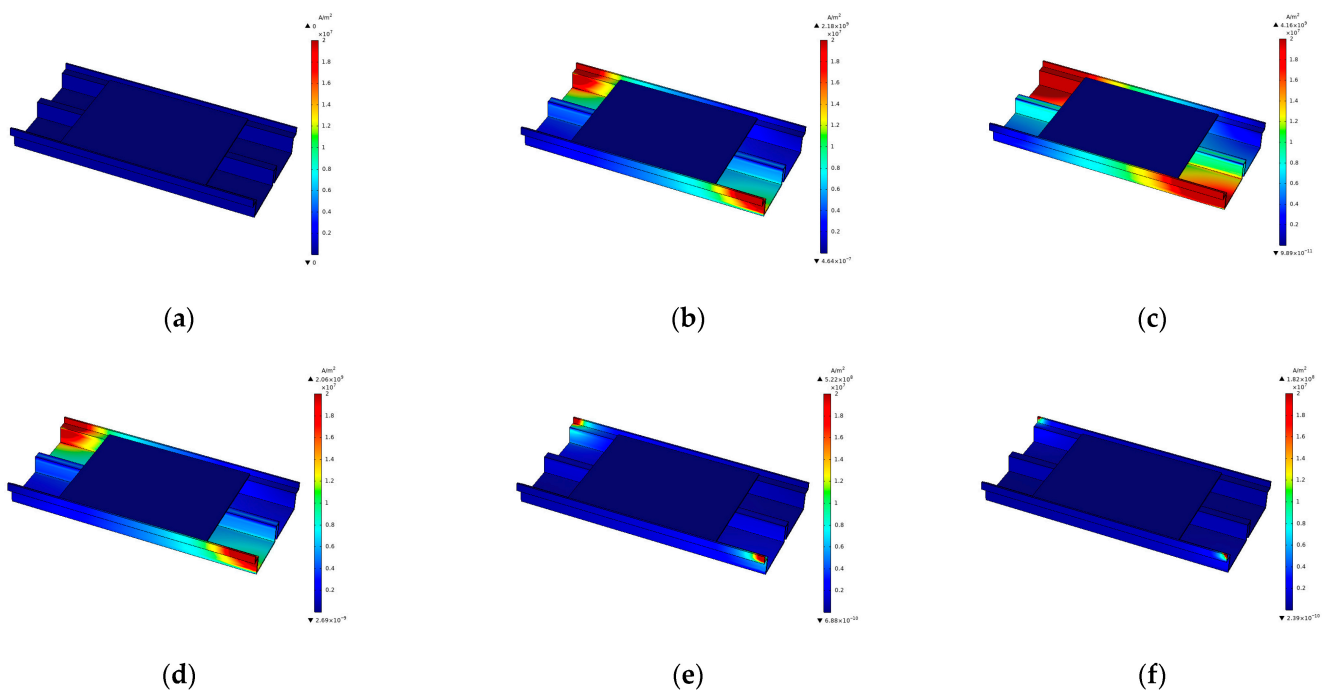
Figure 9. Current transient distribution of BIPV at different times (**a**) 0 µs; (**b**) 2 µs; (**c**) 14 µs; (**d**) 350 µs; (**e**) 1000 µs; (**f**) 1500 µs.

In addition, the temperature rise effect of BIPV during lightning striking is shown in Figure 10. After 1200 µs, the amplitude of lightning current is reduced to 10% I_{imp}. The resistivity of the metal frame is very low and the whole process is transient. Therefore, the temperature rise tends to be stable after 1200 µs. The maximum temperature rise only increases from 0.17 °C to 16.07 °C with increasing lightning current from 10 kA to 100 kA. This temperature rise is easy for the metal frame to withstand without causing any damage.
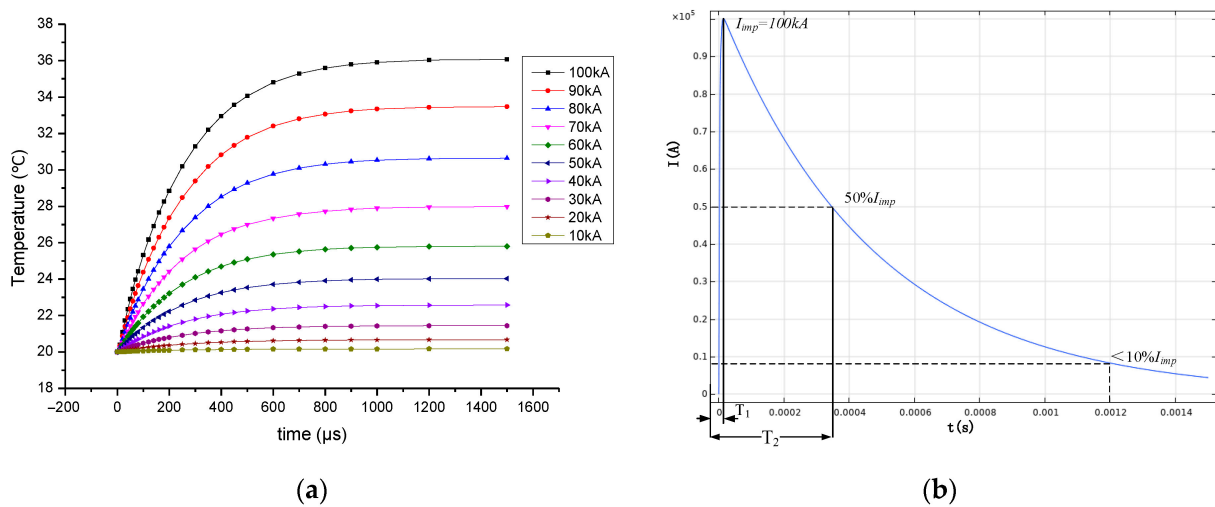
Figure 10. Temperature rise of BIPV at different time and current amplitude. (**a**) The temperature rise of BIPV (**b**) The lightning impulse current waveform.

3.2. Experimental Study

3.2.1. Experimental Method

After multi-physical field simulation analysis, Sample C was selected for experimental verification. As shown in Figure 11, a large current experimental platform for simulating lightning stroke was set up in the laboratory. Sample C was horizontally placed on an insulating table. One copper wire was used to connect the output end of Impulse Current Generator (ICG) to the expected lightning striking point on the metal frame. Another copper wire was used to connect the other end of the metal frame to the grounding electrode.
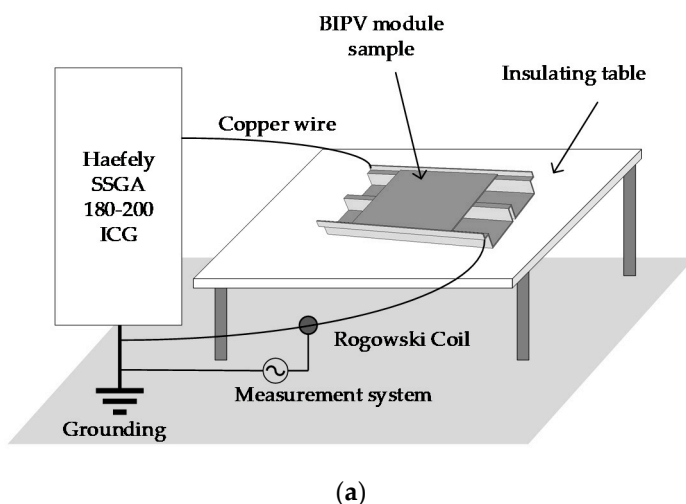
Figure 11. Lightning current withstand performance experiment (**a**) Schematic diagram of experimental platform; (**b**) Layout of experimental setup.

According to the IEC standard [21], the lightning conductor of the highest grade (H-grade) should withstand the impulse current with 100 kA peak value and 2.5 MJ/Ω specific energy, which represents the equivalent energy of the first return stroke component (FRSC) of nature lightning. Since the metal frame of the BIPV module is easy to be struck by lightning, it can function as the lightning receptor on the buildings. The PV module frame should also meet the H-grade impulse current withstand level. In this paper, Haefely SSGA 180–200 ICG was used to output the impulse current with 100 kA peak value and

2.5 MJ/Ω specific energy. Each sample receives three shots. During each shot, the current waveform was measured by a Rogowski coil. The status of the metal frame is observed after each shot to check whether it is damaged.

3.2.2. Experimental Results and Analysis

According to the experimental method of Section 3.2.1, a large impulse current experimental platform was built. The impulse current with amplitude of nearly 100 kA and waveform of 10/350 μs was applied to Sample C by using Haefely SSGA 180–200 ICG. The first impulse current waveform is shown in Figure 12. Table 2 illustrates the parameters of the lightning current in three shots. The waveform of lightning current is defined as T_1/T_2, where T_1 indicates the peak time of lightning current and T_2 indicates the time from the beginning to the attenuation to 1/2 amplitude. Transfer charge Qs is the time integral of lightning current in duration; Specific energy W/R is the time integral of lightning current squared in duration.
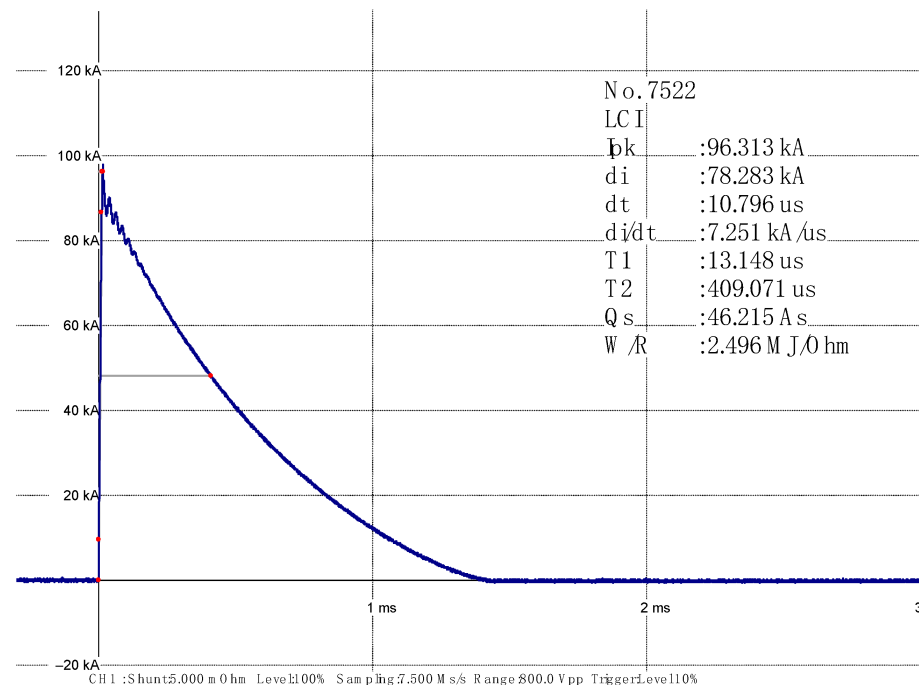

Figure 12. The first impulse current waveform.

Table 2. Impulse current parameter.

No.	Peak Current/kA	T_1/T_2 (μs)	Transfer Charge/As	Specific Energy/(MJ * Ω^{-1})
1	96.313	13.1/409.1	46.251	2496
2	96.508	12.9/397.1	44.674	2426
3	96.938	13.1/400.4	45.073	2451

Due to the impedance of the experimental loop, the impulse currents flowing through the metal frame were a little smaller than 100 kA, i.e., 96.313 kA, 96.508 kA and 96.938 kA respectively. The specific energies of the impulse currents flowing through the metal frame were 2496 MJ/Ω, 2426 MJ/Ω and 2451 MJ/Ω respectively. After three shots, the experimental results showed that the metal frame of Sample C had no signs of deformation and solar cells were not damaged, which was consistent with the results of the thermoelectric coupling analysis model. This shows that the metal frame of BIPV module has adequate lightning energy withstand capability.

4. Conclusions

This paper mainly analyzes the lightning attachment characteristics and lightning energy withstand capability of BIPV modules by numerical simulation and experiment. Two conclusions are drawn as follows,

(a) The electrostatic field model when lightning downward leader above BIPV was built and analyzed with FEM software. An experiment was conducted to verify the numerical analysis. The numerical and experimental study of lightning attachment characteristics shows that the upper edge of the metal frame of BIPV modules is easier to gather charge which can enhance the electric field strength. The electric field strength on the surface of the BIPV module is 132% higher than that of framed double-glass PV module. Therefore, the BIPV module more easily intercepts lightning and the protection efficiency is improved by 114%.

(b) The thermoelectric coupling analysis model is established to solve the potential, current and temperature of lightning BIPV modules during the process of lightning current flows through the metal frame of the BIPV module. The results show that the metal frame of the BIPV modules will not be damaged by the temperature rise of 16.07 °C. In the large impulse current experiment, the metal frame of the BIPV module meets the H-level (the highest level) requirements of the lightning conductor. The BIPV module is not damaged in the experiment which is consistent with the numerical simulation results.

In a word, the metal frame of BIPV can not only intercept lightning stroke to protect the solar cells inside effectively, but can also function as a lightning receptor and down conductor of a building roof. With its good lightning protection performance, BIPV has good application prospects in the rapidly developing distributed PV stations. It has prodigious potential for building integration, especially for less-energy hungry, zero-energy, sustainable, green, and aesthetic building integration. In the future work, our study will focus on the BIPV array on roofs and in facades, evaluating the risk of lightning stroke to BIPV in different application modes. The following research will provide lightning protection methods for green buildings and PV systems.

Author Contributions: Conceptualization, Q.Z. and X.B.; methodology, Q.Z. and X.B.; software, Y.Z. and T.C.; validation, Q.Z. and B.W.; formal analysis, Q.Z. and B.W.; investigation, Y.Z. and T.C.; resources, Q.Z. and B.W.; data curation, X.B.; writing—original draft preparation, Y.Z. and T.C.; writing—review and editing, Q.Z. and Y.Z.; visualization, Y.Z.; supervision, X.B.; project administration, Q.Z. and B.W.; funding acquisition, Q.Z. All authors have read and agreed to the published version of the manuscript.

Institutional Review Board Statement: Not applicable.

Informed Consent Statement: Not applicable.

Data Availability Statement: Not applicable.

Conflicts of Interest: The authors declare no conflict of interest.

References

1. Ghosh, A. Potential of Building Integrated and Attached/Applied Photovoltaic (BIPV/BAPV) for Adaptive Less Energy-Hungry Building's Skin: A Comprehensive Review. *J. Clean. Prod.* **2020**, *276*, 123343. [CrossRef]
2. Chul-Sung, L.; Hyo-mun, L.; Min-joo, C.; Yoon, J. Performance Evaluation and Prediction of BIPV Systems under Partial Shading Conditions Using Normalized Efficiency. *Energies* **2019**, *12*, 273527.
3. Barone, G.; Buonomano, A.; Cesare, F.; Forzano, C.; Giuzio, G.F.; Palombo, A. Passive and active performance assessment of building integrated hybrid solar photovoltaic/thermal collector prototypes: Energy, comfort, and economic analyses. *Energy* **2020**, *209*, 118435. [CrossRef]

4.　Escarre, J.; Li, H.-Y.; Sansonnens, L.; Galliano, F.; Cattaneo, G.; Heinstein, P.; Nicolay, S.; Bailat, J.; Eberhard, S.; Ballif, C.; et al. When PV modules are becoming real building elements: White solar module, a revolution for BIPV. In Proceedings of the 2015 IEEE 42nd Photovoltaic Specialist Conference (PVSC), New Orleans, LA, USA, 14–19 June 2015; pp. 1–2. [CrossRef]

5.　López, C.S.P.; Bonomo, P.; Frontini, F.; Medici, V.; Nespoli, L. Performance assessment of a BIPV Roofing Tile in outdoor testing. In Proceedings of the 2017 IEEE 44th Photovoltaic Specialist Conference (PVSC), Washington, DC, USA, 25–30 June 2017; pp. 2118–2123. [CrossRef]

6.　AlRashidi, H.; Issa, W.; Sellami, N.; Ghosh, A.; Mallick, T.K.; Sundaram, S. Performance Assessment of Cadmium Telluride-Based Semi-Transparent Glazing for Power Saving in Façade Buildings. *Energy Build.* **2020**, *215*, 109585. [CrossRef]

7.　Yu, S.; Xu, W.; Shi, Z. Study on Application of Random Bidirectional Discharge Model in Risk Assessment of Lightning Disaster at Airport. In Proceedings of the 2018 34th International Conference on Lightning Protection (ICLP), Rzeszow, Poland, 2–7 September 2018; pp. 1–4. [CrossRef]

8.　Jiang, T. Electrical Properties Degradation of Photovoltaic Modules Caused by Lightning Induced Voltage. Ph.D. Thesis, Mississippi State University, Starkville, MS, USA, May 2014.

9.　Guo, F.-Y.; Wang, Y.; Huang, M.-D. Design of Photovoltaic Building Lightning Protection Equipment Monitoring and Early Warning System. In Proceedings of the 26th Chinese Control and Decision Conference (2014 CCDC), Changsha, China, 31 May–2 June 2014; pp. 2902–2906.

10.　Fallah, N.; Gomes, C.; Ab Kadir, M.Z.A.; Nourirad, G.; Baojahmadi, M.; Ahmed, R.J. Lightning protection techniques for roof-top PV systems. In Proceedings of the 2013 IEEE 7th International Power Engineering and Optimization Conference (PEOCO), Langkawi, Malaysia, 3–4 June 2013; pp. 417–421. [CrossRef]

11.　Benesova, Z.; Haller, R.; Birkl, J.; Zahlmann, P. Overvoltages in photovoltaic systems induced by lightning strikes. In Proceedings of the 2012 International Conference on Lightning Protection (ICLP), Vienna, Austria, 2–7 September 2012; pp. 1–6. [CrossRef]

12.　Phanthuna, N.; Thongchompoo, N.; Plangklang, B.; Bhumkittipich, K. Model and experiment for study and analysis of Photovoltaic lightning effects. In Proceedings of the 2010 International Conference on Power System Technology, Hangzhou, China, 24–28 October 2010; pp. 1–5. [CrossRef]

13.　Karim, M.R.; Ahmed, M.R. Lightning Effect on a Large-Scale Solar Power Plant with Protection System. In Proceedings of the 2019 1st International Conference on Advances in Science, Engineering and Robotics Technology (ICASERT), Dhaka, Bangladesh, 3–5 May 2019; pp. 1–5. [CrossRef]

14.　Jia, Y.G.; Liu, H.Y.; Su, S.F.; Ding, S.L.; Han, Y.Q.; Liu, Y.; Zhang, X.S. Integrated Photovoltaic System Design and Key Points Analysis Based on Green Building. *Appl. Mech. Mater.* **2014**, *641*, 994–998. [CrossRef]

15.　Guo, F.Y.; Wang, Y.; Huang, M.D.; Yue, W. Fault Tree Establishment of Lightning Protection System Safety of Solar Photovoltaic Building. *Adv. Mater. Res.* **2013**, *860*, 210–213. [CrossRef]

16.　Zaini, N.H.; Ab-Kadir, M.Z.A.; Izadi, M.; Ahmad, N.I.; Radzi, M.A.M.; Azis, N.; Hasan, W.Z.W. On the effect of lightning on a solar photovoltaic system. In Proceedings of the 2016 33rd International Conference on Lightning Protection (ICLP), Estoril, Portugal, 25–30 September 2016; pp. 1–4. [CrossRef]

17.　Cho, J.; Kim, J.; Lee, T.-K.; Kim, K.-H.; Woo, J.-W. Analysis of Lightning Overvoltage According to Position of Lightning-Induced Voltage at the Solar Power Plant. In Proceedings of the 2019 11th Asia-Pacific International Conference on Lightning (APL), Hong Kong, 12–14 June 2019; pp. 1–4. [CrossRef]

18.　Dechthummarong, C.; Thepa, S.; Chenvidhya, D.; Jivacate, C.; Kirtikara, K.; Thongpron, J. Lightning impulse test of field-aged PV modules and simulation partial discharge within MATLAB. In Proceedings of the 2012 9th International Conference on Electrical Engineering/Electronics, Computer, Telecommunications and Information Technology, Phetchaburi, Thailand, 16–18 May 2012; pp. 1–4.

19.　Tamura, K.; Araki, K.; Kumagai, I.; Nagai, H. Lightning test for concentrator photovoltaic system. In Proceedings of the 2011 37th IEEE Photovoltaic Specialists Conference, Seattle, WA, USA, 10–15 June 2011; pp. 000996–000998. [CrossRef]

20.　Coetzer, K.M.; Wiid, P.G.; Rix, A.J. Investigating Lightning Induced Currents in Photovoltaic Modules. In Proceedings of the 2019 International Symposium on Electromagnetic Compatibility—EMC EUROPE, Barcelona, Spain, 2–6 September 2019; pp. 261–266. [CrossRef]

21.　IEC 62561-2:2018. Lightning Protection System Components (LPSC)—Part 2: Requirements for Conductors and Earth Electrodes. Available online: https://webstore.iec.ch/publication/29398 (accessed on 25 January 2018).

22.　Golde, R.H.; Perry, F.R. The frequency of occurrence and the distribution of lightning flashes to transmission lines. *Trans. Am. Inst. Electr. Eng.* **1945**, *64*, 902–910. [CrossRef]

23.　Young, F.S.; Clayton, J.M.; Hileman, A.R. Shielding of transmission lines. *IEEE Trans. Power Appar. Syst.* **1963**, *82*, 132–154.

24.　Love, E.R. Improvements in Lightning Stroke Modeling and Applications to Design of EHV and UHV Transmission Lines. Master's Thesis, University of Colorado, Boulder, CO, USA, 1973.

25.　Whitehead, E.R. Cigre survey of the lightning performance of extra-high-voltage transmission lines. *Electra* **1974**, *33*, 63–89.

26.　Anderson, J.D. *Transmission Line Reference Book-345 kV and above*; Electric Power Research Institute: Palo Alto, CA, USA, 1982; pp. 142–144.

27.　IEEE Std 998-2012, IEEE Guide for Direct Lightning Stroke Shielding of Substations. Available online: https://ieeexplore.ieee.org/document/6656813 (accessed on 30 April 2013).

28. Gamerota, W.R.; Elismé, J.O.; Uman, M.A.; Rakov, V.A. Current waveforms for lightning simulation. *IEEE Trans. Electromagn. Compat.* **2012**, *54*, 880–888. [CrossRef]
29. Berger, K.; Anderson, R.B.; Kroninge, R.H. Parameters of Lighting Flashes. *Electra* **1975**, *41*, 23–37.
30. Bruce, C.E.R.; Golde, R.H. The lightning discharge. *Inst. Elect. Eng.* **1941**, *88*, 487–505.